Density Profile Control with Current Ramping in a Transport Simulation of Ignitor

B. Hu and W. Horton

Institute for Fusion Studies, The University of Texas at Austin, Austin, TX 78712

P. Zhu

Department of Physics and Astronomy,

University of Iowa, Iowa City, IA 52242

F. Porcelli

INFM and Dipartimento di Energetica, Politecnico di Torino, Turin, Italy

(Dated: March 14, 2002)

Abstract

Current ramping to achieve reversed shear (RS) confinement enhancement and peaked density profiles are crucial in achieving ignition conditions in Ignitor. Previous transport simulations used either fixed density profiles or obtained flat density profiles. In this report we explore enhancement confinement, and show a general scheme leading to density profile peaking using the transport model JETTO in the Baldur simulations. In these simulations, peaked density profiles result from the formation of internal transport barrier due to reversed magnetic shear, which is produced by controlled plasma current and volume-averaged density ramping. Such a programmed Ohmic heating scheme is demonstrated to be an effective approach to the ignition of a burning D-T plasma.

I. INTRODUCTION

Several high performance tokamak operating regimes have been achieved in experiments through the peaking of density profiles. These include the improved Ohmic confinement (IOC) regime produced in ASDEX [1], the pellet enhanced performance (PEP) mode in Alcator C Tokamak and JET, and the supershot mode in TFTR. In these tokamak regimes, the peaked core density profiles bring down the $\eta_{\rm i}(= d\ln T_{\rm i}/d\ln n_{\rm i})$ value below the critical threshold for ion temperature gradient (ITG) mode, and help to produce internal transport barriers by generating the large shear radial electric field, which is required for turbulence suppression, through the deep density gradient. In addition to enhancing the confinement, peaked density profiles are also necessary for optimizing the fusion reaction rate and alpha heating power of a tokamak plasma, and when combined with centrally peaked temperature profile, would help to reach the ignition condition early. It is thus desirable to seek and analyze the density profile control schemes that effectively lead to density profile peaking in transport simulations of burning plasma experiments on machines such as Ignitor.

Previous simulations of Ignitor experiments either simply utilized density profiles with fixed peaking shape [2] or obtained flat density profiles when the self-consistent evolution of which was allowed [3]. Efforts have been made to increase core plasma density by pellet injection in Ignitor simulation, however, the density profile peaking seems to only last for a very short period [4]. In this report, we demonstrate in transport simulation the scheme of producing peaked density profile through current ramping, which eventually leads to the ignition of Ignitor plasma when sawtooth event is avioded. The basic mechanism is that plasma current ramping with sufficient rate and proper timing generates a non-monotonic q profile with reversed magnetic shear (RS) during the evolution of magnetic flux surface. An internal transport barrier forms in the reversed shear region which, combined with the properly programmed tokamak edge gas puffing, produces a central peaked plasma density profile in a timely manner. Since the reversed magnetic shear is a natural by-product of rapid plasma current ramping as well as a well confirmed mechanism in the formation of transport barrier, such a scheme of density profile peaking is intrinsic to the Ohmic heating process as in Ignitor, and independent of the particular transport model used in simulations.

Reversed magnetic shear (RS) plasma confinement has become one of the main approaches to achieving fusion grade plasmas in tokamaks. An example of using the current

ramp in an Ohmic tokamak to produce an internal transport barrier (ITB) is the Tore Supra current ramp experiment [5]. In this experiment a high current ramp-up rate defined by $\omega_{\rm ramp} = d\ln I_{\rm p}/dt \sim 10{\rm s}^{-1}$ is used to create a reversed shear plasma with $I_{\rm p}$ increasing from 0.4 MA to 1.2 MA. After the formation of the RS configuration the ICRH auxiliary heating power is applied with a time profile that ramps up to 4 MW starting at the time $I_{\rm p}$ reaches its maximum value 1.2 MA. In the following steady state phase the density is maintained by gas fueling at $0.65n_{\rm G}$ ($n_G = I({\rm MA})/\pi a^2$, the Greenwald density) and the electron transport barrier is maintained for 2s. In this 2s period ($\geq 50\tau_E$) there is a reduced level of the fluctuations and a 50% increase of the global energy confinement time. This scenario is similar to the one used here to reach ignition except that alpha heating is used in place of the RF heating.

Here, the transport model JETTO is used as a standard model in simulations to demonstrate the scheme. JETTO is an empirical model with a mixed Bohm and gyro-Bohm scaling. It has been bench-marked in various confinement regimes with experimental data from several different tokamak machines [6]. Even though, it is still uncertain whether or not the transport scaling in JETTO could be applied to the compact tokamak regime with high magnetic field, high density and high current. However, the issue of extrapolation of transport models should not digress our purpose here in an essential way, due to the universal nature of the current ramping scheme.

The rest of the paper is organized as follows. In section II we briefly review the transport model used, and describe in detail the simulation scheme. Simulation results are presented and analyzed in section III. Finally in section IV, the summary and discussion are given.

II. TRANSPORT MODEL AND SIMULATION SCHEME

Here we have adopted the transport model JETTO in our simulations of Ignitor. JETTO is an empirical model containing several extensions to the Taroni-Bohm electron thermal transport model originally developed for JET L-mode experiments [7]. Erba *et al.* [8] first extended the Taroni-Bohm model to ion thermal transport and to the Ohmic regime. By adding edge temperature gradient dependence, Erba *et al.* [9] further extended their model to H-mode regimes with transient and nonlocal effects. Later a gyro-Bohm transport term was included to account for experimental results on other tokamak devices with various

sizes [6]. In the final model of JETTO, the thermal diffusivities of electrons and ions take the form [10]

$$\chi_{\rm e,i} = \chi^{\rm B}_{\rm e,i} + \chi^{\rm gB}_{\rm e,i} \qquad \text{Bohm term + gyro-Bohm term} \tag{1}$$

$$\chi^{\rm B}_{e,i} = \alpha^{\rm B}_{\rm e,i} \frac{cT_{\rm e}}{eB} \frac{q^2 a}{L_{pe}} \left\langle L^*_{T_{\rm e}} \right\rangle^{-1}_{\Delta V} \qquad \text{Bohm term} \tag{2}$$

$$\chi^{\rm gB}_{\rm e,i} = \alpha^{\rm gB}_{\rm e,i} \frac{cT_{\rm e}}{eB} \frac{\rho_{\rm si}}{L_{T\rm e}} \qquad \text{gyro-Bohm term} \tag{3}$$

where $\left\langle L^*_{T_{\rm e}} \right\rangle^{-1}_{\Delta V} = |(T_{\rm e}(x=0.8) - T_{\rm e}(x=1))/T_{\rm e}(x=1)|$ is the correction factor for non-locality at the edge, $L_{pe} = |d\ln p_{\rm e}/dr|^{-1}$ and $L_{T\rm e} = |d\ln T_{\rm e}/dr|^{-1}$ are the electron pressure and electron temperature gradient scale length, respectively, $\rho_{\rm si}$ is ion Larmor radius at the electron temperature, and the adopted values of the empirical transport coefficients are

$$\alpha_{\rm Be} = 8\times 10^{-5}, \quad \alpha_{\rm Bi} = 2\alpha_{\rm Be}$$

$$\alpha_{\rm gBe} = 3.5\times 10^{-2}, \ \alpha_{\rm gBi} = \alpha_{\rm gBe}/2$$

as bench-marked from data in ITER and Tore Supra databases. The particle diffusivity of main gas ion species is modeled as

$$D_{\rm i} = \left[c_1 + (c_2 - c_1)\frac{r}{a}\right] \frac{\chi_{\rm e}\chi_{\rm i}}{\chi_{\rm e} + \chi_{\rm i}}, \tag{4}$$

where $c_1 = 1$ and $c_2 = 0.3$ are empirical coefficients and r/a is the normalized minor radius of device. Formulas (2) and (3) have no critical gradient and give transport for all non-vanishing $\nabla T_{\rm e}$. There are theoretical and experimental reasons to revise these formulas to include a critical gradient. The electron turbulent transport has shown clear evidence of a critical gradient in the ASDEX [11] and Tore Supra [12]. The role of the critical gradient and the associated turbulent particle pinch deserves close examination in our future work.

Weak and reversed magnetic shear has been shown to suppress several dominant MHD and microinstabilities in tokamak, particularly those driven by unfavorable geodestic magnetic curvature [13–17]. Such suppression leads to the reduced turbulent transport accross the reversed shear region, resulting in the formation of internal transport barrier. In tokamak experiments with transport barriers, reversed shear works either alone or together with some other turbulence suppression mechanisms, such as the $\mathbf{E}\times\mathbf{B}$ flow shear. The mechanism of reversed shear is incorporated into the JETTO model in a simple way, by reducing the transport coefficients in reversed shear region. In particular, the Bohm contribution to

the transport is allowed to go zero whenever the magnetic shear becomes negative. Similar approach of implementing the RS and $\mathbf{E} \times \mathbf{B}$ flow shear effects has been adopted in some earlier simulations of ITBs in tokamaks [18], and may suffice in an empirical transport model as well as for the purpose here.

In the simulation, we choose the global design parameters based on the specification given in Coppi *et al.* [19]. The relevant initial and boundary conditions for the transport equations are slected as following. The initial central temperatures for both ions and electrons are set to be 1 keV, and the initial central density is chosen to be $3.0 \times 10^{20}\mathrm{m}^{-3}$ for both deuterium and tritium. During the heating process, the edge temperature increases from 0.3 keV at the beginning to 2.0 keV in the end [3], while the edge density remains a constant value of $1.0 \times 10^{20}\mathrm{m}^{-3}$ for both Deuterium and Tritium ion species.

The key procedure of the Ohmic heating scheme in our simulation is the plasma current ramping. The time histories of plasma current and volume density for a reference simulation run #ignif01 with peaked density profile are shown in Fig. 1. The plasma current I_p is rapidly increased from its initial value during the first second, to its target maximum steady value of 12 MA by the end of the ramping stage, drops to 11 MA, and then remains there for the rest of the heating process. With a fixed target value of plasma current and a fixed length of ramping period, the average current ramping rate is determined by the initial plasma current. We found that in order to have negative magnetic shear during the time evolution of magnetic flux surfaces, the initial plasma current should be approximately equal to or less than 4 MA. This corresponds to a threshold for the plasma current ramping rate of 7 MA/s approximately.

The rapid ramping of plasma current is accompanied by a gradual growth of electron volume-average density starting from $4.0 \times 10^{20}\mathrm{m}^{-3}$ towards its target value of $9.0 \times 10^{20}\mathrm{m}^{-3}$, controlled by neutral gas puffing from edge (Fig. 1). For a given ramping rate of plasma current, there is an upper limit for density ramping rate above which the desired density profile peaking or plasma ignition would not occur. Too low a rate of density ramping, on the other hand, would also delay or even prevent ignition. A staged ramping scheme for volume averaged density with ramping rates carefully chosen between the two opposite ends could ensure the peaking of density profile as well as an early ignition, as, for example, in the reference case in Fig. 1.

III. SIMULATION RESULTS

With the transport model and simulation scheme presented in previous section, peaked density profiles are obtained during early time stages (prior to ignition) of reference simulation run #ignif01. In Fig. 1 we show the optimal current and density ramp that we have found to date. During this time the Ohmic power increases to its maximum of 39 MW as shown in Fig. 1. The peak of the Ohmic power reduced just at the end of the current ramp. The alpha power is at about 40 KW at this time and will continue to increase rapidly as seen in Fig. 1.

The radial electron density profiles at 6 representive time slices are plotted in Fig. 3d, in comparison with those of corresponding time slices in Fig. 4d from an earlier simulation run (#ignia010) with less current ramping rate [3]. The peaking of density radial profile is evident in the reference case #ignif01 times prior to ignition, characterized by an inward moving internal transport barrier. Following Coppi *et al.* [2], we also use the ratio of the central density to the volume-averaged density $n_{\rm e}(0)/\langle n_{\rm e}\rangle$ to quantatize the peakness of the density profile. In Fig. 2, we compare the time evolution of the density profile peakness $n_{\rm e}(0)/\langle n_{\rm e}\rangle$ of the two simulation cases. The correlation between the current ramping rate and the density profile peakness is apparant for time stages prior to ignition.

The peaked density profile seen in our simulations is basically a direct consequence of the formation of internal transport barrier, produced indirectly by rapid current ramping through reversed magnetic shear. Such a mechanism of density peaking can be clearly demonstrated by the causal relations among the time-evolving radial profiles of several transport quantities, including plasma current density j_z, the safety factor q, the particle diffusivity $D_{\rm i}$, the electron density $n_{\rm e}$, the ion thermal conductivity $\chi_{\rm i}$, and the ion temperature $T_{\rm i}$ for the reference simulation run #ignif01 in Fig. 3. Initial plasma density and temperature radial profiles spread flatly. During the fast current ramping stage when poloidal magnetic flux sinks in from boundary, most of the plasma current accumulates around plasma edge if the current ramping rate beats the diffusion rate of the magnetic flux. As a result the safety factor profile is also dipped between the core and the edge as does that of Ohmic heating power deposition. The reversed shear leads to the suppression of both particle and thermal transport in that region, forming steep gradients in both density and temperature profiles there, namely, an internal transport barrier. As the plasma is heated up, the re-

versed shear region and the transport barrier both move inward, resulting in the peaking of density profile. The timing and location of reversed shear region and the transport barrier are well correlated in profiles in Fig. 3. As a comparison, the corresponding process in the earlier simulation run #ignia010 is shown in Fig. 4, where neither the RS region or the ITB is present.

The favorable effects of density profile peaking on ignition was demonstrated earlier in Coppi *et al.* [2]. However, our studies here differ from those of Coppi *et al.* in that the peaked density profile in our transport simulations are produced dynamically by plasma current ramping instead of being prescribed artificially. As found in our simulations, plasma with peaked density profile during the heating process could reach ignition condition earlier than the time when sawtooth is triggered, which ensures the ignition. In Fig. 5 we compare the time traces of α-heating power P_α and the total confinement power loss P_L for those simulation runs shown in Fig. 2 with two different levels of density profile peaking due to different plasma current ramping rates. The ignition, defined as the moment when the α-heating power P_α is balanced by the total thermal loss P_L, can be seen to occur at $t = 4.24$ s in simulation #ignif01 with density profile peaking, where the sawtooth oscillation starts at $t = 4.34$ s. In simulation runs with less current ramping rate, sawtooth events kick in earlier than the time when the ignition conditions could be met, which prevent ignition from occuring.

IV. SUMMARY

The simulations reported in previous section demonstrate a scheme of obtaining a peaked density profile during the heating process of Ignitor through the formation of internal transport barrier by rapid plasma current ramping. At the initial stage of Ohmic heating, plasma current density would accumulate around the edge if the ramping rate of the total plasma current exceeds its inward diffusion rate. A minimum point in the profile of the safety factor q appears where the plasma current density accumulates, forming a region with reversed magnetic shear. An internal transport barrier is thus produced in that region due to the suppression of fluctuation by reversed and weak magnetic shear there. Following the inward movement of the transport barrier as the plasma current sinks inside further, a peaked density as well as temperature profile is obtained. Peaked denisty and temperature profiles,

as resulted from transport barrier, enable the Ignitor plasma to reach ignition condition earlier than the occurence of sawtooth events, hence ensure the achievement of ignition. Although the JETTO transport model is used in our simulations, such a density profile peaking scheme is in principle independent of the particular choice of transport model, since it derives from the instrinsic feature of Ohmic heating process of Ignitor experiment and the universal mechanism of transport barrier formation due to reversed magnetic shear.

Recent experiments in ASDEX [11] and Tore Supra [12] clearly show that the radial electron thermal flux is described by

$$\begin{aligned} q_{\rm e} &= -n_{\rm e}\chi_{\rm e}[\nabla T_{\rm e} - (\nabla T_{\rm e})_{\rm c}] \\ &= -n_{\rm e}\chi_{\rm e} + n_{\rm e}T_{\rm e}v_r \end{aligned}$$

where the second equivalent form of the heat flux driven by the gradient excess over the critical gradient $(T_{\rm e})_{\rm c}$ defines the inward thermal pinch velocity $v_r = -\chi_{\rm e}/L_{\rm c}$ where $L_{\rm c}^{-1} \equiv -(\nabla T_{\rm e})_{\rm c}/T_{\rm e}$. These off-diagonal transport terms are an intrinsic part of the symmetries that occurs in the turbulent transport matrices [20]. Experimental evidence for other anomalous pinch terms is found in particle balance and angular momentum balance. In our future work we will show the necessicity of a particle pinch term $\Gamma = -D(dn_{\rm e}/dr) + nv_r$ associated with the turbulent particle flux, as well as the effect of these two off-diagonal terms on the Ignitor simulation.

Acknowledgments

This work was supported by the U.S. Dept. of Energy Contract No. DE-FG03-96ER-54346. We would like to thank Dr. Bateman and Dr. Kritz for providing the code and the initial simulation run.

[1] F. X. Söldner, E. R. Müller, F. Wagner, H. S. Bosch, A. Eberhagen, H. U. Fahrbach, G. Fussmann, O. Gehre, K. Gentle, J. Gernhardt, *et al.*, Physical Review Letters **61**, 1105 (1988).

[2] B. Coppi, M. Nassi, and L. E. Sugiyama, Physica Scripta **45**, 112 (1992).

[3] W. Horton, F. Porcelli, P. Zhu, A. Aydemir, Y. Kishimoto, and T. Tajima, Nuclear Fusion **42**, 169 (2002).

[4] C. N. Nguyen, *Predictive transport simulations for Ignitor* (2000), unpublished.

[5] G. T. Hoang, C. Bourdelle, X. Garbet, G. Antar, R. V. Budny, T. Aniel, V. Basiuk, A. Becoulet, P. Devynck, J. Lasalle, *et al.*, Physical Review Letters **84**, 4593 (2000).

[6] M. Erba, T. Aniel, V. Basiuk, E. Becoulet, and X. Litaudon, Nuclear Fusion **38**, 1013 (1998).

[7] A. Taroni, M. Erba, E. Springman, and F. Tibone, Plasma Physics and Controlled Fusion **36**, 1629 (1994).

[8] M. Erba, V. Parail, E. Springmann, and A. Taroni, Plasma Physics and Controlled Fusion **37**, 1249 (1995).

[9] M. Erba, A. Cherubini, V. Parail, E. Springmann, and A. Taroni, Plasma Physics and Controlled Fusion **39**, 261 (1997).

[10] M. Erba, G. Bateman, A. H. Kritz, and T. Onjun, *Subroutine for computing particle and energy fluxes using the mixed transport model* (1999), unpublised.

[11] F. Ryter, F. Leuterer, G. Pereverzev, H.-U. Fahrbach, J. Stober, W. Suttrop, and A. U. Team, Physical Review Letters **86**, 2325 (2001).

[12] G. T. Hoang, C. Bourdelle, X. Garbet, G. Giruzzi, T. Aniel, M. Ottaviani, W. Horton, P. Zhu, and R. V. Budny, Physical Review Letters **87**, 125001 (2001).

[13] C. Kessel, J. Manickam, G. Rewoldt, and W. M. Tang, Physical Review Letters **72**, 1212 (1994).

[14] F. Levinton, M. Zarnstorff, S. Batha, M. Bell, R. Bell, R. Budny, C. Bush, Z. Chang, E. Fredrickson, A. Janos, *et al.*, Physical Review Letters **75**, 4417 (1995).

[15] E. Strait, L. Lao, M. Mauel, B. W. Rice, T. S. Taylor, K. H. Burrell, M. S. Chu, E. A. Lazarus, T. H. Osborne, S. J. Thompson, *et al.*, Physical Review Letters **75**, 4421 (1995).

[16] M. A. Beer, G. W. Hammett, G. Rewoldt, E. J. Synakowski, M. C. Zarnstorff, and W. Dorland, Physics of Plasmas **4**, 1792 (1997).

[17] Y. Kishimoto, J.-Y. Kim, W. Horton, T. Tajima, M. J. LeBrun, and H. Shirai, Plasma Physics and Controlled Fusion **41**, A663 (1999).

[18] V. Parail, Y. Baranov, C. Challis, G. Cottrell, B. Fischer, C. Gormezano, G. Huysmans, X. Litaudon, A. Sips, F. Sldner, *et al.*, Nuclear Fusion **39**, 429 (1999).

[19] B. Coppi, A. Airoldi, F. Bombarda, G. Cenacchi, P. Detragiache, C. Ferro, R. Maggiora, L. Sugiyama, and G. Vecchi, *Critical physics issues for ignition experiments: Ignitor*, report Report PTP 99/06, MIT (RLE) (September 1999).

[20] H. Sugama, M. Okamoto, W. Horton, and M. Wakatani, Physics of Plasmas **3**, 2379 (1996).

TABLES

TABLE 1. **Global parameters for Ignitor simulation.**

major radius	minor radius	elongation	triangluarity	toroidal field
R (m)	a (m)	κ	δ	B_{T}
1.32	0.47	1.83	0.43	13

FIGURE CAPTIONS

FIG. 1. Time history of a) plasma current $I_{\rm p}$, b) volume-average density $\langle n_{\rm e} \rangle$, c) Ohmic power $P_{\rm oh}$ and α power P_α, and d) confinement time $\tau_{\rm E}$ in the reference simulation run #ignif01 with peaked density profile.

FIG. 2. Comparison of time evolutions of density profile peakness $n_{\rm e}(0)/\langle n_{\rm e} \rangle$ for two simulation runs with different current ramping rate.

FIG. 3. Radial profiles of a) plasma current density j_z, b) safety factor q, c) particle diffusivity D_i, d) electron density $n_{\rm e}$, e) ion thermal conductivity χ_i, and f) ion temperature T_i, at six time slices $t = 0, 1, 2, 3, 4$ and 5 s in the reference simulation run #ignif01.

FIG. 4. Radial profiles of a) plasma current density j_z, b) safety factor q, c) particle diffusivity D_i, d) electron density $n_{\rm e}$, e) ion thermal conductivity χ_i, and f) ion temperature T_i, at six time slices $t = 0, 1, 2, 3, 4$ and 5 s in the reference simulation run #ignia010.

FIG. 5. Time traces of α-heating power P_α and the total confinement power loss P_L in those three simulation runs shown in Fig. 5.

FIGURES

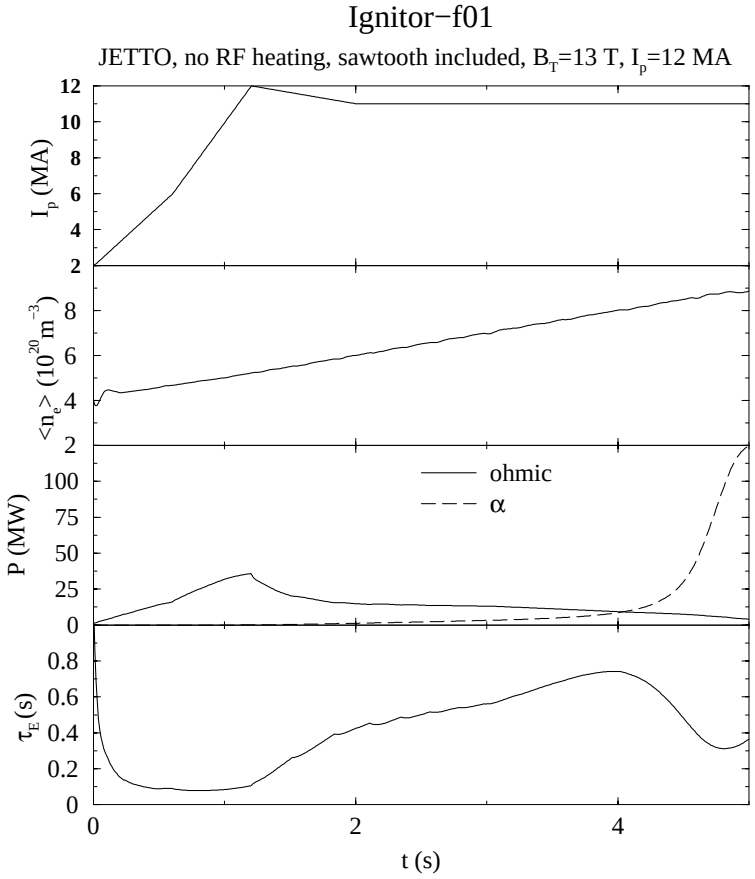

FIG. 1.

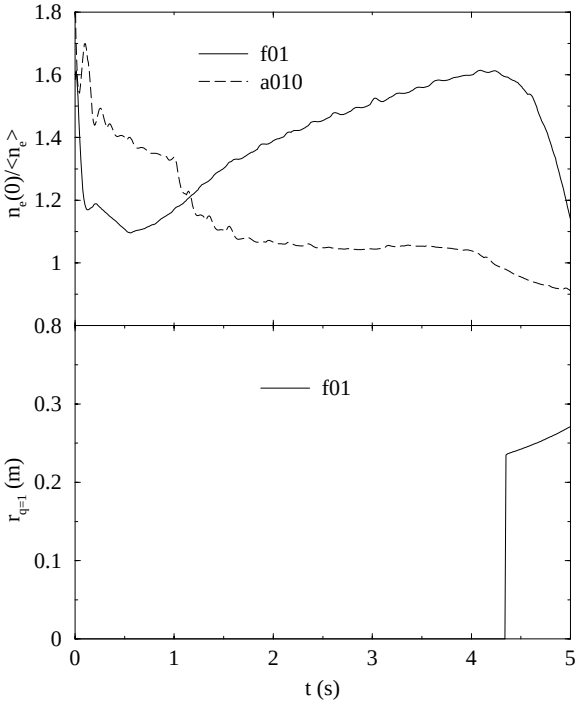

FIG. 2.

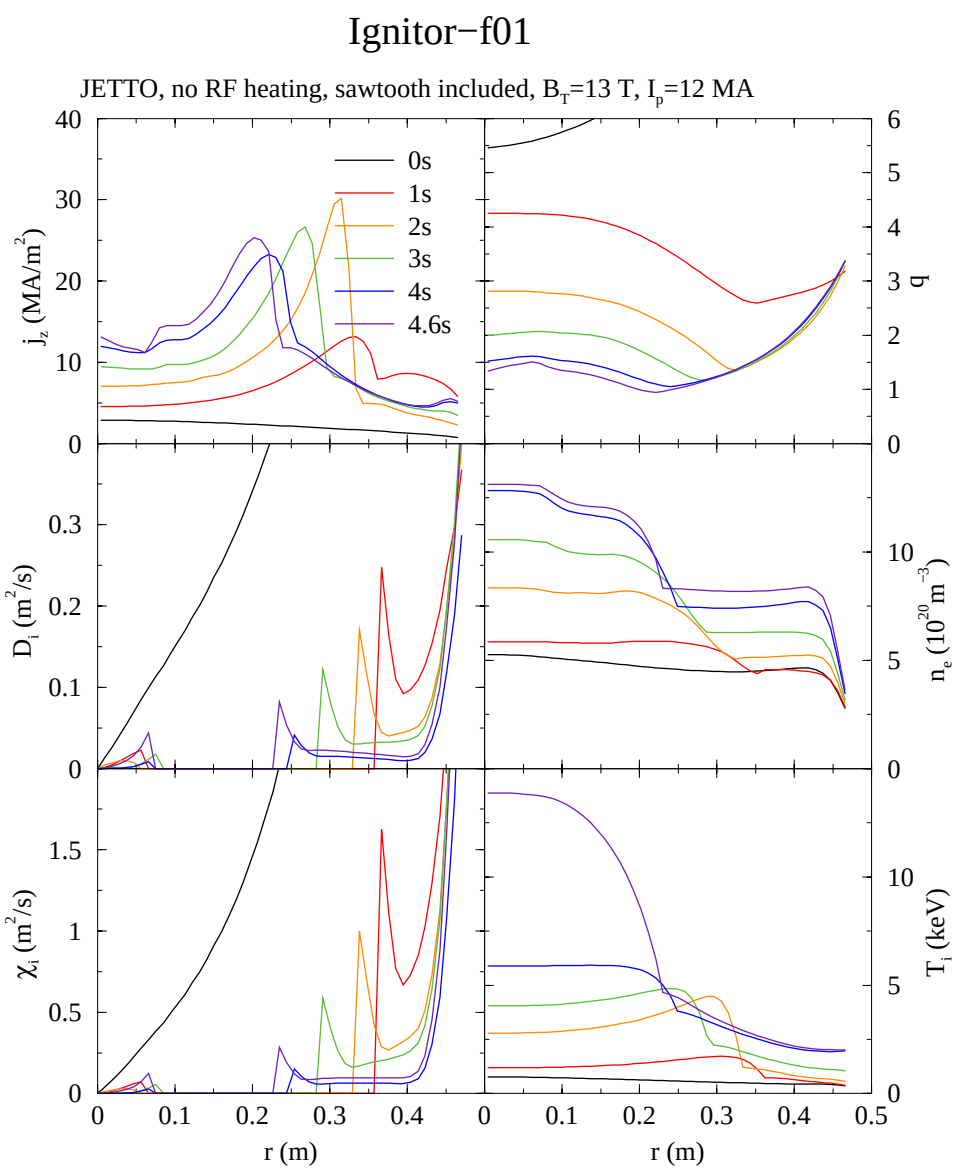
Ignitor−f01
JETTO, no RF heating, sawtooth included, B_T=13 T, I_p=12 MA
0s
1s
2s
3s
4s
4.6s
j_z (MA/m^2)
q
D_i (m^2/s)
n_e (10^20 m^-3)
χ_i (m^2/s)
T_i (keV)
r (m)
r (m)

FIG. 3.

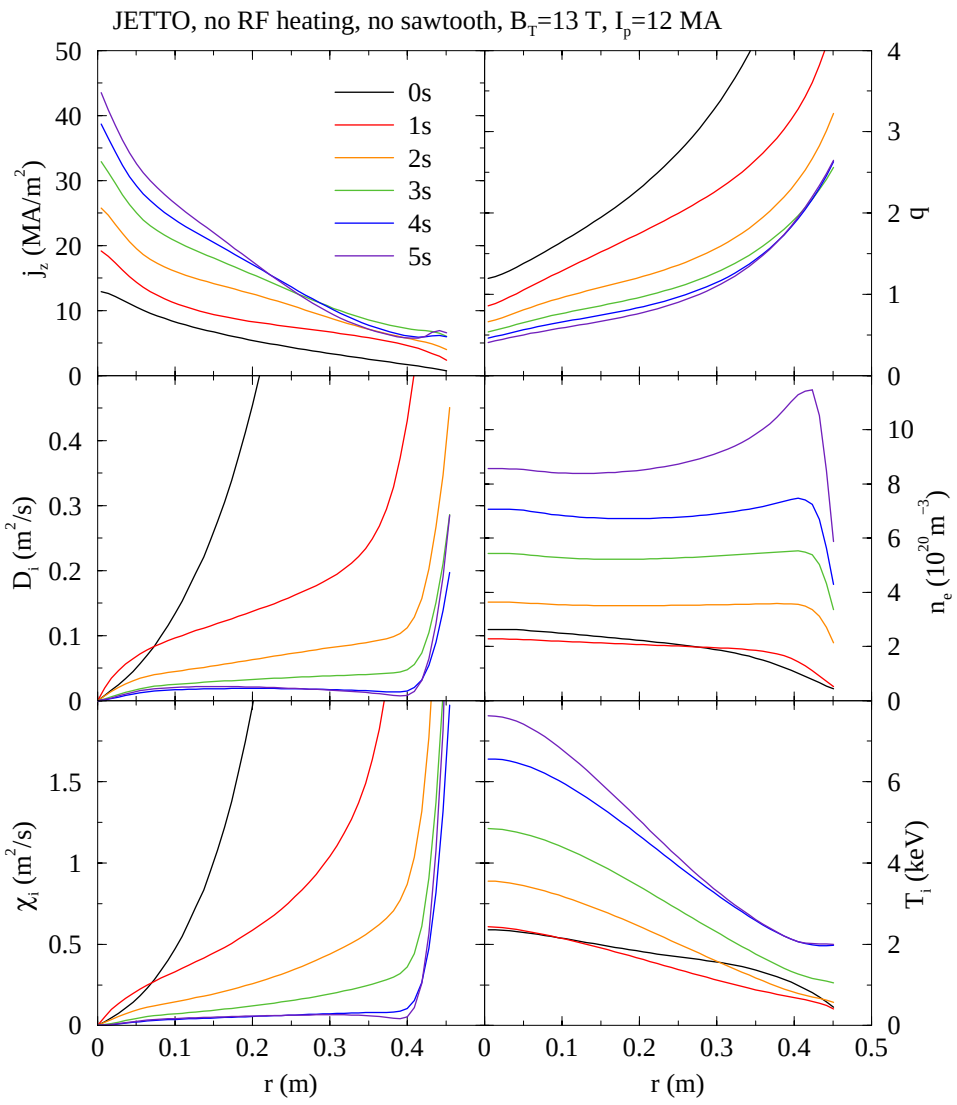
Ignitor−a10
JETTO, no RF heating, no sawtooth, B_T=13 T, I_p=12 MA
0s
1s
2s
3s
4s
5s
j_z (MA/m^2)
q
D_i (m^2/s)
n_e (10^20 m^-3)
χ_i (m^2/s)
T_i (keV)
r (m)
r (m)

FIG. 4.

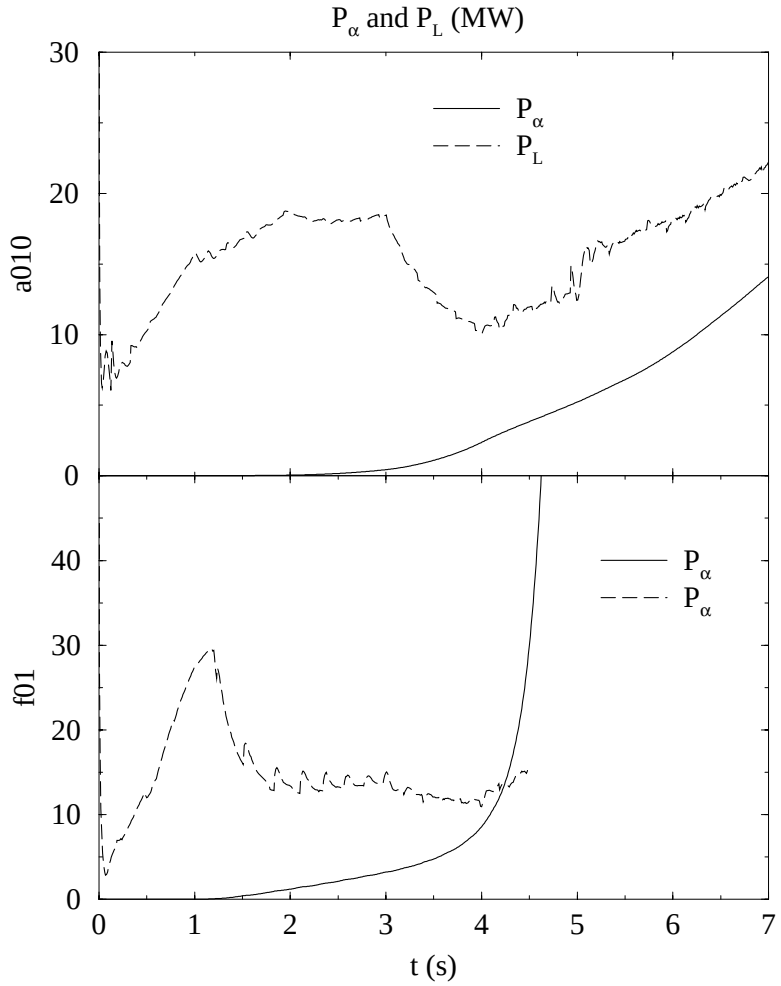

FIG. 5.